OXFORD

Mechanically Induced Nuclear Shuttling of β-Catenin Requires Co-transfer of Actin

Buer Sen[1], Zhihui Xie[1], Sean Howard[2], Maya Styner[1] (iD), Andre J. van Wijnen[3], Gunes Uzer[2], Janet Rubin[1] (iD),*

[1]Department of Medicine, University of North Carolina, Chapel Hill, NC, USA
[2]Department of Mechanical and Biomedical Engineering, Boise State University, Boise, ID, USA
[3]Department of Biochemistry, University of Vermont Medical School, Burlington, VT, USA
*Corresponding author: Janet Rubin, Department of Medicine, University of North Carolina, Chapel Hill, NC 27599, USA. Email: jrubin@med.unc.edu

Abstract

Mesenchymal stem cells (MSCs) respond to environmental forces with both cytoskeletal re-structuring and activation of protein chaperones of mechanical information, β-catenin, and yes-associated protein 1 (YAP1). To function, MSCs must differentiate between dynamic forces such as cyclic strains of extracellular matrix due to physical activity and static strains due to ECM stiffening. To delineate how MSCs recognize and respond differently to both force types, we compared effects of dynamic (200 cycles × 2%) and static (1 × 2% hold) strain on nuclear translocation of β-catenin and YAP1 at 3 hours after force application. Dynamic strain induced nuclear accumulation of β-catenin, and increased cytoskeletal actin structure and cell stiffness, but had no effect on nuclear YAP1 levels. Critically, both nuclear actin and nuclear stiffness increased along with dynamic strain-induced β-catenin transport. Augmentation of cytoskeletal structure using either static strain or lysophosphatidic acid did not increase nuclear content of β-catenin or actin, but induced robust nuclear increase in YAP1. As actin binds β-catenin, we considered whether β-catenin, which lacks a nuclear localization signal, was dependent on actin to gain entry to the nucleus. Knockdown of cofilin-1 (*Cfl1*) or importin-9 (*Ipo9*), which co-mediate nuclear transfer of G-actin, prevented dynamic strain-mediated nuclear transfer of both β-catenin and actin. In sum, dynamic strain induction of actin re-structuring promotes nuclear transport of G-actin, concurrently supporting nuclear access of β-catenin via mechanisms used for actin transport. Thus, dynamic and static strain activate alternative mechanoresponses reflected by differences in the cellular distributions of actin, β-catenin, and YAP1.

Key words: YAP-signaling protein; actin cytoskeleton; nuclear transport; mesenchymal stem cell; mechanical stress.

Graphical Abstract
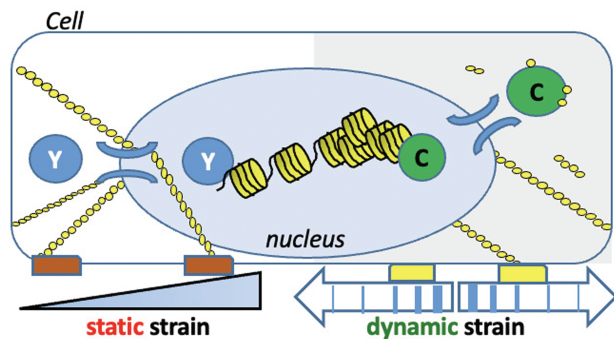
β-Catenin (C) entry into the nucleus due to dynamic strain is dependent on actin transport. YAP (Y) nuclear entry depends on a static actin-LINC structure delivering force to open nuclear pores.

Significance Statement

Cells integrate both static and dynamic mechanical signals through the actin cytoskeleton, which is attached to the nuclear envelope, affecting nuclear transport of β-catenin and YAP1. Dynamic strain induces nuclear translocation of β-catenin, but not YAP1, while static strain causes nuclear translocation of YAP1, but not β-catenin. Importantly, nuclear transport of actin is induced by dynamic but not static force. Furthermore, nuclear import of β-catenin depends on cofilin/importin-9 dependent actin transport mechanisms. Thus the presence of β-catenin and YAP1 in the nucleus represent specific responses to regulatory mechanical signals.

Introduction

Mechanical information, both extrinsic and intrinsic to the cell, regulates proliferation, differentiation and function. β-Catenin and YAP1 are mechanoresponsive proteins that modulate these processes in mesenchymal stem/stromal cells (MSCs).[1-3] β-Catenin nuclear localization occurs after dynamic strain,[1,4-6] which concurrently induces actin rearrangement into F-actin cables which arch over the nucleus[7] and connect to the inner nuclear membrane through actin's association with the Linker of Nucleoskeleton and Cytoskeleton (LINC) complex.[8] YAP1 nuclear translocation is also modulated by cytoskeletal actin fibers which form in response to forces generated after adherence to stiff substrates[2] but has not been studied with respect to dynamic strain. Static strain, in turn, has not been shown to effect rapid nuclear β-catenin transfer.[9] Overall, how the cell regulates nuclear import of β-catenin and YAP1 in response to acute application of dynamic or static mechanical force is poorly defined.

Both mechanoresponsive molecules, β-catenin and YAP1, lack nuclear localization signals (NLS) in their primary structure[10,11] and are subject to phosphorylations guiding their disposition. For example, phosphorylation of β-catenin by GSK3β targets it for proteasomal degradation,[4] while phosphorylation of YAP1 by LATS1/2 leads to its exclusion from the nucleus.[12] Mechanical force, through AKT-mediated phosphorylation of GSK3β, inhibits β-catenin turnover and enhances nuclear import.[4,13] However, these phosphorylation events do not fully explain nuclear transfer engendered by mechanical force. YAP1 nuclear import through nuclear pores is enhanced by actin cables which develop after static strain.[14] In turn, when F-actin connections to the nuclear actin cap decrease due to mechanical unloading (eg, simulated microgravity), nuclear YAP1 levels decrease.[15,16] The actin cytoskeleton that forms after dynamic strain also connects to the nucleus via LINC, where β-catenin positions itself for entry.[17] While this might suggest that entry of β-catenin into the nucleus is also consequent to cytoskeletal actin structure, nuclear localization of YAP1 and β-catenin separate after cytochalasin D induced disruption of actin polymerization: cytochalasin D leads YAP1 egress, but promotes nuclear accumulation of β-catenin.[18] It thus appears that nuclear translocation of β-catenin in response to dynamic force is achieved through a fundamentally distinct mechanism than that controlling the entry of YAP1.

Biomechanical forces are represented by a continuum. In bone, MSC within the bone marrow cavity respond to dynamic applied forces as expected during exercise, as well as to local static forces conveyed by MSC localization on hard mineralized tissue. The emerging organizational and functional complexity of bone marrow microenvironments enabled by recent technologies such as CLARITY,[19] single-cell sequencing,[20] and tracing studies[21] suggest that site-specific mechanical information contributes to the functioning and structural organization of these niches. As such movement of a stromal cells within bone marrow, or changes in matrix stiffness during fracture repair may provide physiological static forces to cells. During high physical activity, such as running, bone surfaces where bone cells, including MSCs reside are exposed to dynamic deformations up to 2000-3500 microstrains (με).[22] Furthermore, the removal of dynamic force promotes MSC adipogenesis.[1,23] As such, bone and other tissues respond to these forces by integrating distinct types of biophysical input

that differ in frequency (periodicity) and amplitude (magnitude) in a manner that depends on biological and cellular contexts.[24] YAP1-related mechanoresponses have been largely examined as a late response to changes in the static modulus of the substrate on which cells adhere,[2,14] while β-catenin has been studied as an acute response to dynamic strain regimens.[25] The responses of YAP1 and β-catenin together were examined in a canine kidney cell line in which altered modulus was replaced with a single biaxial stretch of high magnitude.[26] This type of force application resulted in the translocation of both mechanosensory proteins to the nucleus from prior sites in the cytoplasm (YAP1) or cell-cell contacts (β-catenin). In these epithelial cells, YAP1 moved rapidly into the nucleus, but β-catenin nuclear entry required at least 6 hours. The activation of both proteins was associated with entry into the cell cycle, similar to the cell cycle response of MSC to β-catenin nuclear entry.[27] The latter findings suggest functional specialization or perhaps redundancy in how mechanoresponders might regulate cell proliferation.

Because both β-catenin[28,29] and YAP1[30] lack classic NLS we postulated that assessment of their responses to distinct mechanical forces would offer clues to mechanisms of nuclear transfer. The results presented here show that both β-catenin and YAP1 respond to acute application of strain but exhibit differences with respect to periodicity of the mechanical signal. Furthermore, nuclear actin content increased after dynamic strain, but not static, strain. Importantly, we found that nuclear entry of β-catenin depends on concurrent nuclear entry of actin. In sum, mechanically induced nuclear entry of β-catenin differs from that of YAP1 as it is independent of cytoplasmic actin structure, depending instead on mechanisms of nuclear actin transport.

Methods

Materials

Fetal bovine serum was from Atlanta Biologicals (Atlanta, GA). Culture media, trypsin-EDTA reagent, antibiotics from Sigma-Aldrich (St. Louis, MO). Other commercial reagents include 1-oleoyl lysophosphatidic acid (LPA; cat# 62215) from Caymen Chemical (Ann Arbor, MI), 6-well BioFlex Collagen-I coated plates (cat# BF-3001C) from Flexcell International (Burlington, NC), Ibidi USA μ-Slide chamber (cat#: NC0515977) from Fisher (Hampton, NH).

Cells and Culture Conditions

Mouse marrow-derived MSCs were harvested from C57BL/6J murine bone marrow using a validated protocol,[31] (IACUC approved). We have previously described these cells, which contain no hematopoietic elements, as capable of generating both osteoblasts and adipocytes.[32] Cells isolated using this exact protocol express all relevant mRNA biomarkers expected of MSCs based on RNA-seq data presented previously.[33] Cells were maintained in minimal essential medium containing 10% FBS, 100 μg/mL penicillin/streptomycin. For adipogenic differentiation, primary bone marrow derived murine MSCs were seeded on BioFlex culture plates at 10 000 cells per well 2 days prior to addition of adipogenic media (5 μg/mL insulin, 0.1 μM Dexamethasone, and 50 μM Indomethacin). For immunofluorescence staining, MSCs were plated at a density of 2000 (β-catenin) or 10 000 (YAP1) cells/cm² and cultured for 1 day before application of treatments.

For YAP1 staining, the cells were cultured in adipogenic medium (0.1 μM dexamethasone, 50 μM indomethacin, and 5 μg/mL insulin) overnight before mechanical loading or reagent treatment.

RNA Interference

Cells were transfected with siRNA (25-50 nM) in serum-free OptiMEM overnight before replacing the medium and adding reagents for cell treatment, using the Life Technology protocol for Lipofectamine RNAiMAX (cat #13778150). RNA interference studies were performed with siRNAs for Ipo9: 5′- CCCAGCUCUUCAACCUGCUUAUGGA and control (nucleotide change within same sequence) 5′-CCCTCTCC TAACCGTTCATTGAGGA; Cfn1: 5′-AAACTAGGTGGCAG CGCCGTCATTT and the control 5′- TCATTTCCCTGGA GGGCAAGCCTTT.

Application of Mechanical Forces

Uniform biaxial strain was applied to MSCs plated at 10 000 cells per well on 6-well Bioflex Collagen-I-coated plates using the Flexcell FX6000T system (Flexcell International, Hillsborough, NC). The dynamic mechanical strain conditions were as previously shown to activate β-catenin[7] and consisted of 2% dynamic strain at 10 cycles per minute for 20 minutes (200 cycles). The static strain regimen, utilizing the same plates, strain and instrument was designed with after[26] and consisted of 2% static strain applied for 3 hours continuously (1 cycle; stretch and hold). Cells were incubated overnight in media as noted in experiments prior to being subjected to either dynamic strain (2% × 200 cycles) or static strains (2% continuously × 1 cycle).

Measurement of Cell and Nuclear Modulus

For cell modulus measurement, the silicon base of the culture plate was excised with a scalpel after Flexcell strain treatment. Specimens were carefully transferred to the lid of a 35mm culture plate for analysis by atomic force microscopy (AFM). Nuclei were isolated from strain plates using a NE-PER nuclear isolation kit (Thermo Scientific) according to manufacturer protocols. Force-displacement curves for both intact MSC nuclei and isolated nuclei were acquired using a Bruker Dimension FastScan Bio AFM. MLCT-SPH-5 µm-DC-A probes were used to decrease variables in calculating moduli. These probes are produced with a consistent 5 um silicon nitride tip and factory calibrated, using laser Doppler vibrometry, spring constants. To fully calibrate the probes, the deflection sensitivity was measured immediately prior to each experiment by ramping on sapphire and averaging 5 measurements. Mesenchymal stem cells and nuclei were located using the AFM's optical microscope and engaged on using a minimal force set point (1-3 nN) to ensure contact while minimizing applied force and resultant deformation prior to testing. Ramps were performed over the approximate center of each nucleus for all samples. After engaging on a selected nucleus to ensure probe/nucleus contact as described above, force curve ramping was performed at a rate of 2 µm/s over 2 µm total travel (1 µm approach, 1 µm retract). Five replicate force-displacement curves with an indentation depth of ~500 nm were acquired and saved for each nucleus tested, with at least 3 s of rest between ramps.

Measured force-displacement curves were analyzed assuming Hertzian (spherical contact) mechanics.[34] AtomicJ, an open source program for analyzing AFM data, was used to automatically fit the force-displacement curves and calculate the modulus.[35] Poisson's ratio 0.4 was used as a best estimate for the effective Poisson's ratio of the cells. The modulus of each individual sample was reported as the average of at least 5 consecutive force curve measurements. Group averages were then obtained from the average values for the individual samples.

Immunofluorescence Microscopy

Cells were fixed with 4% paraformaldehyde for 10 minutes, permeabilized in 0.1% Triton-X 100 for 5 minutes, and blocked with 5% donkey serum for 30 minutes. Three consecutive washes for 10 minutes with phosphate-buffered saline (PBS) were performed between each step. Silicone membranes were cut from plates and transferred to 6-well plate surface. Incubation with primary antibodies at 37 °C for 1 hour included goat β-catenin antibody (cat# AB0095) from OriGene Biotechnologies (Rockville, MD) and rabbit YAP1 antibody (cat# 14074) from Cell Signaling (Danvers, MA). Visualization of primary antibodies was performed with Cy5 conjugated donkey anti-goat (for β-catenin; cat# 705-175-147) and Rhodamine Red-conjugated anti-rabbit (for YAP1; cat# 711-295-152). These secondary antibodies were obtained from Jackson Immuno Research (West Grove, PA). Actin stress fibers were examined using Alexa Fluor 488-conjugated phalloidin (cat# A12379; Lifetechnologies). After 3 consecutive 10-minute washes with PBS, membranes were sealed with mounting medium on glass or the cells in chamber slides were covered with PBS. For 3D images, cells were examined using a model LSM 880 confocal microscope (Zeiss, Thornwood, NY).

Real Time RT-PCR

Total RNA was isolated with the RNeasy plus mini kit (Qiagen; Germantown, MD). Reverse transcription of 1 µg of RNA in a total volume of 20 µL was performed with iScript cDNA Synthesis Kit (Bio-Rad) prior to real time PCR (iCycler; Bio-Rad, Hercules, CA). 25-µL amplification reactions contained primers (0.5 µM), dNTPs (0.2 mM each), 0.03 units Taq polymerase, and SYBR-green (Molecular Probes, Eugene, OR) at 1:150 000. Aliquots of cDNA were diluted 5 to 5000-fold to generate relative standard curves to which sample cDNA was compared. *Cfl1* forward primer: 5′-cgcaagtcttcaacaccaga-3′ and reverse primer: 5-ttgtctggcagcatcttgac-3′. *Ipo9* forward primer: 5′-tggattcggatggagaagtc-3′ and reverse primer: 5′-agtaaatgagctcgggcaga-3′. Standards and samples were run in triplicate. PCR products were normalized to 18 S amplicons in the RT sample, and standardized on a dilution curve from RT sample.

Nuclear and Cytoplasmic Protein Fractionation

Cells were washed with 1× PBS, cell pellets resuspended in 0.33 M sucrose, 10 mM HEPES, pH 7.4, 1 mM MgCl$_2$, 0.1% Triton X-100 (pellet vs buffer volume, 1:5) and placed on ice for 15 minutes. After 3000 rpm for 5 minutes, the supernatant was collected (cytoplasmic fraction). Pellets were resuspended in 0.45 M NaCl and 10 mM HEPES, pH 7.4, and placed on ice for 15 minutes. After centrifugation at 12 000 rpm for 5 minutes, the nuclear fraction supernatant was collected.

Immuno-precipitation Analysis

Mesenchymal stem cells were transfected with recombinant plasmid vectors that express either a chimeric actin protein fused to fluorescent YFP and a NLS peptide or the YFP-NLS

control protein. Cells were separated into cytoplasmic and nuclear compartments fractions that were incubated with GFP antibody (cat# 2555, Cell Signaling) which recognizes the YFP protein. Immuno-complexes were bound to Protein A/G beads and recovered by low-speed micro centrifugation at 3000 rpm (approximately 1000×*g*) for 30 s at 4 °C. After final wash, pellets were resuspended in PBS for SDS-PAGE analysis.

Immunoblot Analysis

Fractionated proteins were loaded onto a 7%-10% poly-acrylamide gel for chromatography and transferred to polyvinylidene difluoride membrane. After blocking, primary antibody was applied overnight at 4 °C including antibodies against β-catenin (cat# AB0095-200, OriGene), β-Actin (cat# 4967, Cell Signaling), GFP (cat#2555, Cell Signaling), PARP1 (cat# sc-365315, Santa Cruz Biotechnology, Dallas, TX,) or LDHA (cat# 2012, Cell Signaling). Secondary antibody conjugated with horseradish peroxidase was detected with ECL plus chemiluminescence kit (Amersham Biosciences/GE Healthcare, Piscataway NJ). The images were acquired with an HP Scanjet and densitometry determined using NIH ImageJ, 1.37v.

Statistical Analysis

The results are expressed as means ± SEM. For comparisons, 1-way analysis of variance or *t* test (GraphPad Prism). Experiments were replicated at least twice to assure reproducibility. Densitometry data, where given, were compiled from at least 3 separate experiments. AFM experiments were repeated 3 times. *P*-values of <.05 were considered significant.

Results

Dynamic and static strains both increase cell stiffness, yet have different effects on mechanoresponders β-catenin and YAP1

YAP1's mechanoresponse has been studied after plating on substrates of high stiffness (>40 ,kPa), as noted in bone marrow MSC, mammary epithelial and HeLa cervical carcinoma cells.[2] YAP1 also responds to a single stretch of 15% within a 2-hour time frame in MDCK kidney epithelial cells.[26] In contrast, application of physiologically relevant dynamic strain (200 cycles ×2%) to bone marrow MSCs induces rapid nuclear transfer of β-catenin.[4,36] Here we compared the specific responses of β-catenin and YAP1 with physiological levels of dynamic and static strains in mouse MSCs. Application of 200 cycles of 2% strain is referred to here as "dynamic" strain, while a similar magnitude strain, applied and held at 2%, is referred to as "static" strain. Phalloidin staining showed an increase in F-actin in both dynamic and static conditions at 3 hours (Fig. 1A). In order to measure changes in cell stiffness, MSCs treated with either dynamic or static strain along with non-strain controls were tested under an atomic force microscope to measure live cell modulus as we have previously reported.[37] On average, application of dynamic strain increased the AFM-measured cell modulus by 22% compared with non-strained controls and 11% compared with static strain, while static strain resulted in a 13% increase compared with non-strained controls (Fig. 1B).

At 3 hours after application of dynamic strain, increases in nuclear β-catenin across the cell population were significant. The static condition induced much less, but still significant β-catenin nuclear transfer (Fig. 1C). Analysis of β-catenin immunofluorescence (IF) signal over multiple nuclei and similar areas of cytoplasm, revealed the magnitude of this effect (143 ± 5.9% vs 108 ± 3.6% for dynamic and static strain respectively, compared with control, Fig. 1D).

To assess YAP1 in MSCs, cell confluence was increased to ensure that YAP1 could be clearly detected in the cytoplasm (Fig. 1E). Both static and dynamic strain induced a similar increase in the F-actin cytoskeleton. However, while dynamic strain had only marginal effects on YAP1 nuclear accumulation by 3 hours, static strain robustly induced nuclear transfer of YAP1 (128 ± 2.2% vs 178 ± 3.3% for dynamic and static respectively, compared to control, Fig. 1E, F). Hence, dynamic and static strain had qualitatively different effects on the mechanoresponses of β-catenin and YAP1.

Nuclear Actin Increases After Dynamic Strain

Increased nuclear transfer of YAP1 associated with plating cells on substrates of high modulus is thought to require release of YAP1 from actin monomers.[38] Accordingly, depolymerization of cytoplasmic F-actin in MSCs by cytochalasin D results in YAP1 exit from the nucleus. In direct contrast, β-catenin enters the nucleus after F-actin depolymerization.[18] The cytochalasin D effect on either mechanoresponder is complicated by mass transport of depolymerized actin monomers from the cytosol into the nucleus; increased levels of nuclear actin, which represents a substrate for nuclear members of the actin toolbox, can support re-polymerization and perhaps modulate nuclear modulus.[39] For this reason, we investigated whether differences in actin response to dynamic and static strains could affect β-catenin or YAP1 nuclear entry.

To localize cellular actin after dynamic and static strain, both of which induce F-actin polymerization in the cytoplasm,[36,40,41] we examined the subcellular localization of a chimeric actin protein fused to fluorescent YFP and a NLS peptide. As expected, the YFP-NLS peptide lacking actin was entirely confined to the nucleus and was insensitive to either dynamic or static strain (Supplementary Fig. S1). Fusion of the actin protein to the NLS-YFP protein module resulted in considerable redistribution of YFP to the cytoplasm irrespective of the NLS signal (Fig. 2A). This finding firmly established that the NLS-YFP-actin fusion protein was not restricted to the nucleus. These results indicated that the NLS-YFP-labeled actin protein remained subject to regulators of actin transport and that its cellular localization was partially governed by molecular regulatory mechanisms that control actin entry and exit from the nucleus. After dynamic strain, actin accumulated in the nucleus, in stark contrast to the static condition where the YFP-actin signal did not increase (Fig. 2A). Both strain conditions consistently induced cytoplasmic actin polymerization, as evidenced by actin cables containing the YFP-actin-NLS molecule. Western blot assessment of YFP-actin showed nuclear accumulation after dynamic strain, but not after static strain (Fig. 2B, C).

Actin is known to bind β-catenin/E-cadherin complexes[42] and when artificially increased in the nucleus, F-actin associates with β-catenin, enhancing its binding to cell cycle regulator genes (ie, c-myc, cyclin D, OCT4).[43] After dynamic strain, we measured an increase in nuclear YFP-actin, as well as in the β-catenin associated with the epitope used for immunoprecipitation (Fig. 2D). As predicted, IP for β-actin pulled down β-catenin in MSCs, and IP for β-catenin pulled
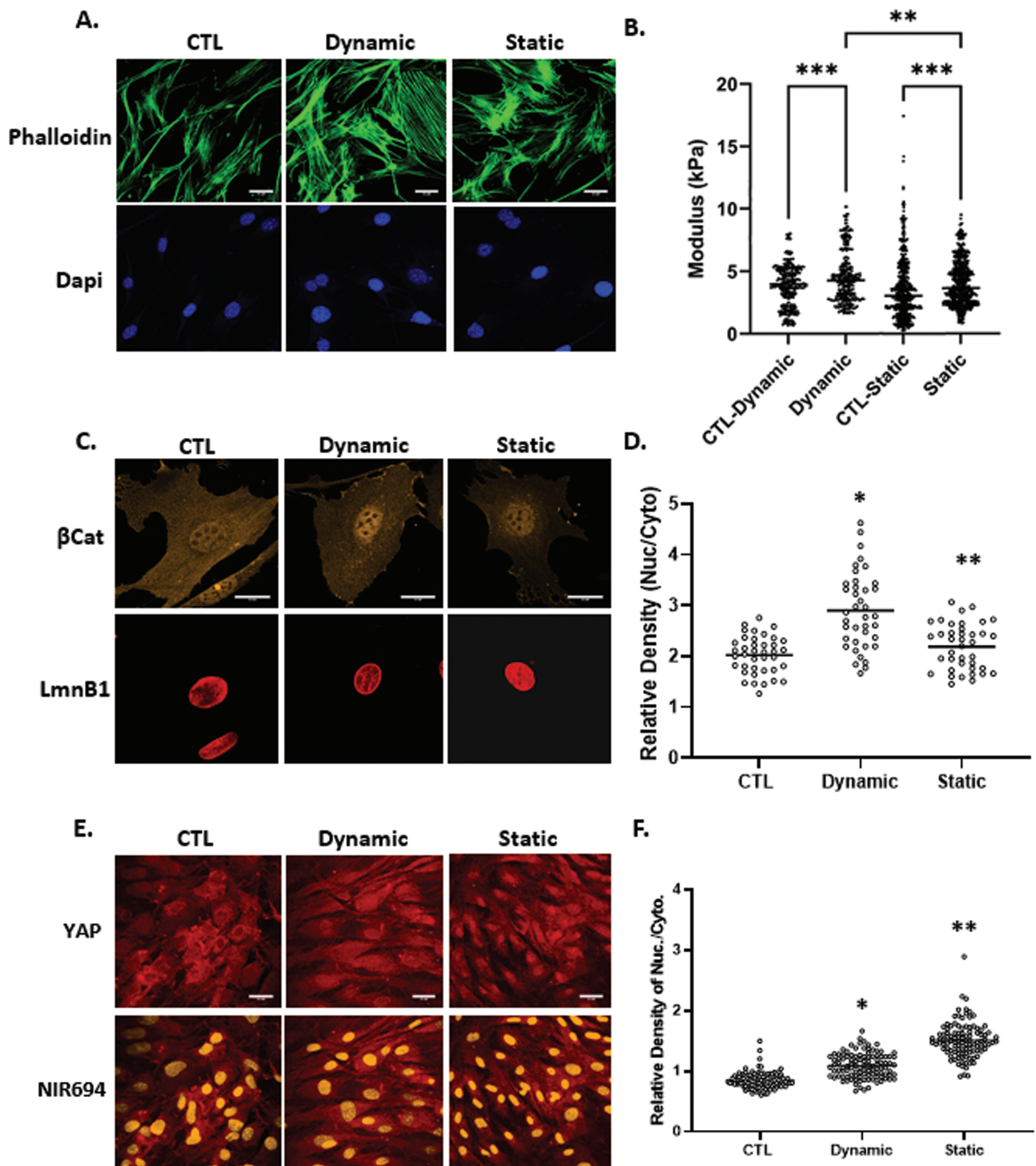
Figure 1. Dynamic and static strains both increase cell stiffness yet have different effects on mechanoresponders. Mesenchymal stem cells were seeded in minimal essential medium at a density of 2000 or 10 000 cells/cm^2 for β-catenin or YAP1 experiments respectively. Twenty-four hours later, application of 2% dynamic (200 cycles over 20 minutes) or static strain (2% and hold tension) was followed by staining with phalloidin (green), anti-β-catenin (yellow), or anti-YAP (red), scale bar = 25 μm (**A, D,** and **E**). Nuclear intensity of β-catenin and YAP1 was analyzed by ImageJ program and statistical significance indicated by letter a and b, both of them $P < .0001$ and * ≠ ** (**D** and **F**). (**b**) Application of dynamic strain increased the AFM-measured cell modulus by 22% ($P < .001$, $N = 350$/grp) compared with non-strained control and while static strain resulted in a 13% increase compared with non-strained control ($P < .0001$, $N = 800$/grp). Cell modulus of MSCs treated with dynamic strain were, on average, 11% larger compared with static strain groups ($P < .05$).

down actin (Fig. 2E). Shown in Fig. 2F, both strain regimens increased the nuclear modulus: dynamic strain increased nuclear modulus 2-fold ($P < .001$) compared with control, and 1.3-fold ($P < .001$) compared with static strain. Static strain increased nuclear modulus by 1.5-fold ($P < .01$) compared with its own control.

Repeated episodes of mechanical force application may sustain and increase effects observed for a single period of
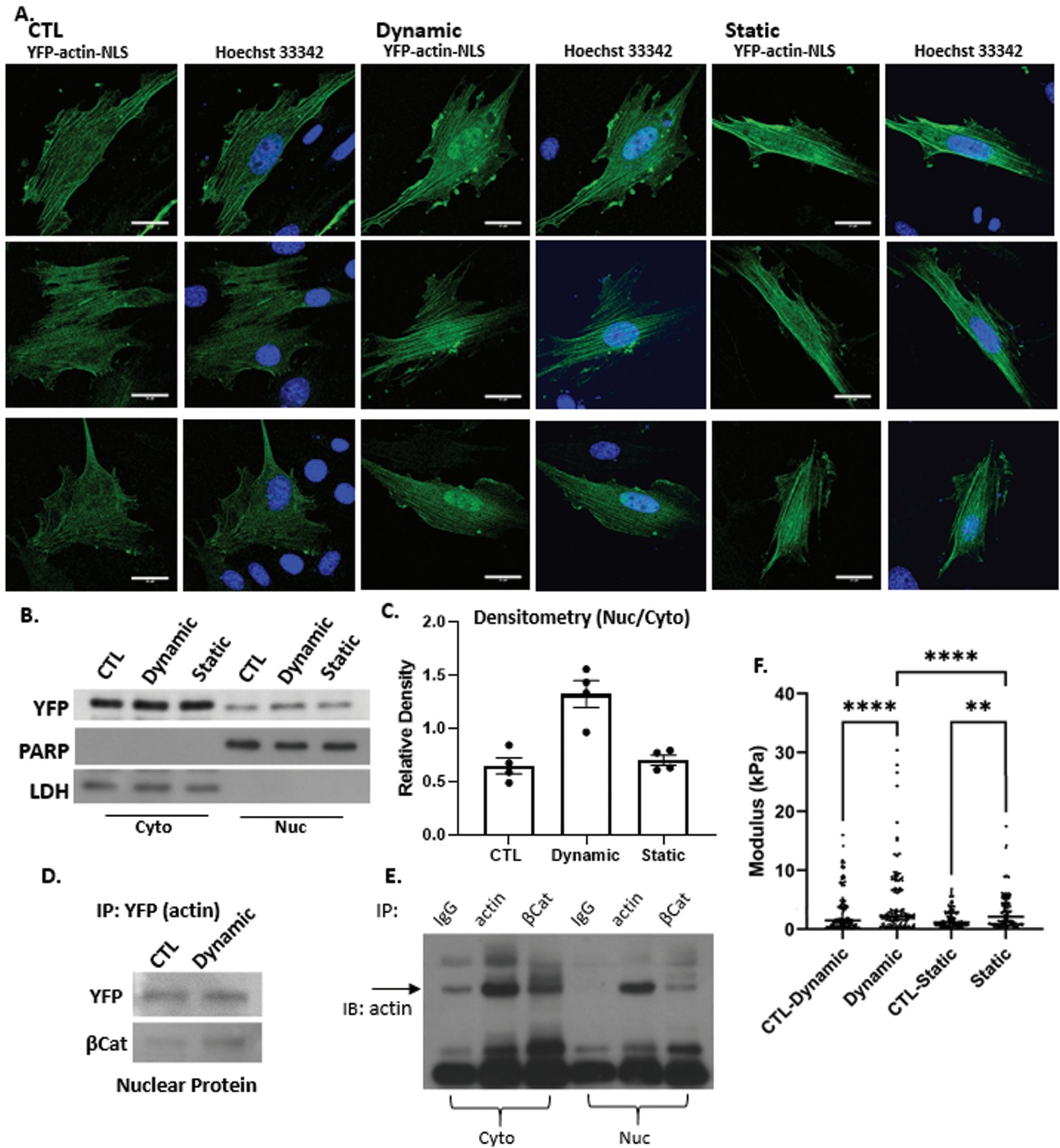
Figure 2. Nuclear actin increases after dynamic strain. Nuclear YFP-NLS-βActin in MSC increases after dynamic, but not static strain (3 examples of each condition shown, scale bar = 25 μm (**A**). Western blot of cytoplasmic and nuclear lysates (**B**) was quantified by densitometry $n = 4$, $P < .005$ (**C**). IP nuclear protein using anti-GFP and IB YFP and β-catenin shows association between the 2 molecules (**D**). Cell cytoplasmic and nuclear lysates were IP for IgG, actin or βCat and immunoblotted for actin (**E**). AFM-measured modulus of isolated nuclei showed that dynamic strain increased the nuclear modulus by 2-fold ($P < .001$) compared to control and 1.3-fold compared with static strain groups ($P < .001$). Static strain increased nuclear modulus by 1.5-fold compared with control ($P < .05$) (**F**).

mechanical stimuli. As such, we applied a second bout of dynamic strain delivered 3 hours after the first bout (Fig. 3A), a time when augmentation of the F-actin cytoskeleton has plateaued.[7] Micrographic analysis revealed that this force re-application regimen further enhanced β-catenin localization in the nucleus (Fig. 3B,C), consistent with previous observations.[36] The increased level of nuclear β-catenin was clearly reflected by increased immunofluorescence after the second strain bout (Supplementary Fig. S1, third column). Quantitation revealed a significant 30%-40% increase in YFP-actin after the first stimulus ($136 \pm 2.7\%$ compared with control at 100%), and 65%-75% after the second episode of strain ($170 \pm 3.5\%$ compared with control) as shown in Fig. 3C. Immunoprecipitation of the YFP-actin-NLS fusion protein using a GFP antibody revealed that YFP-actin forms stable protein/protein complexes with
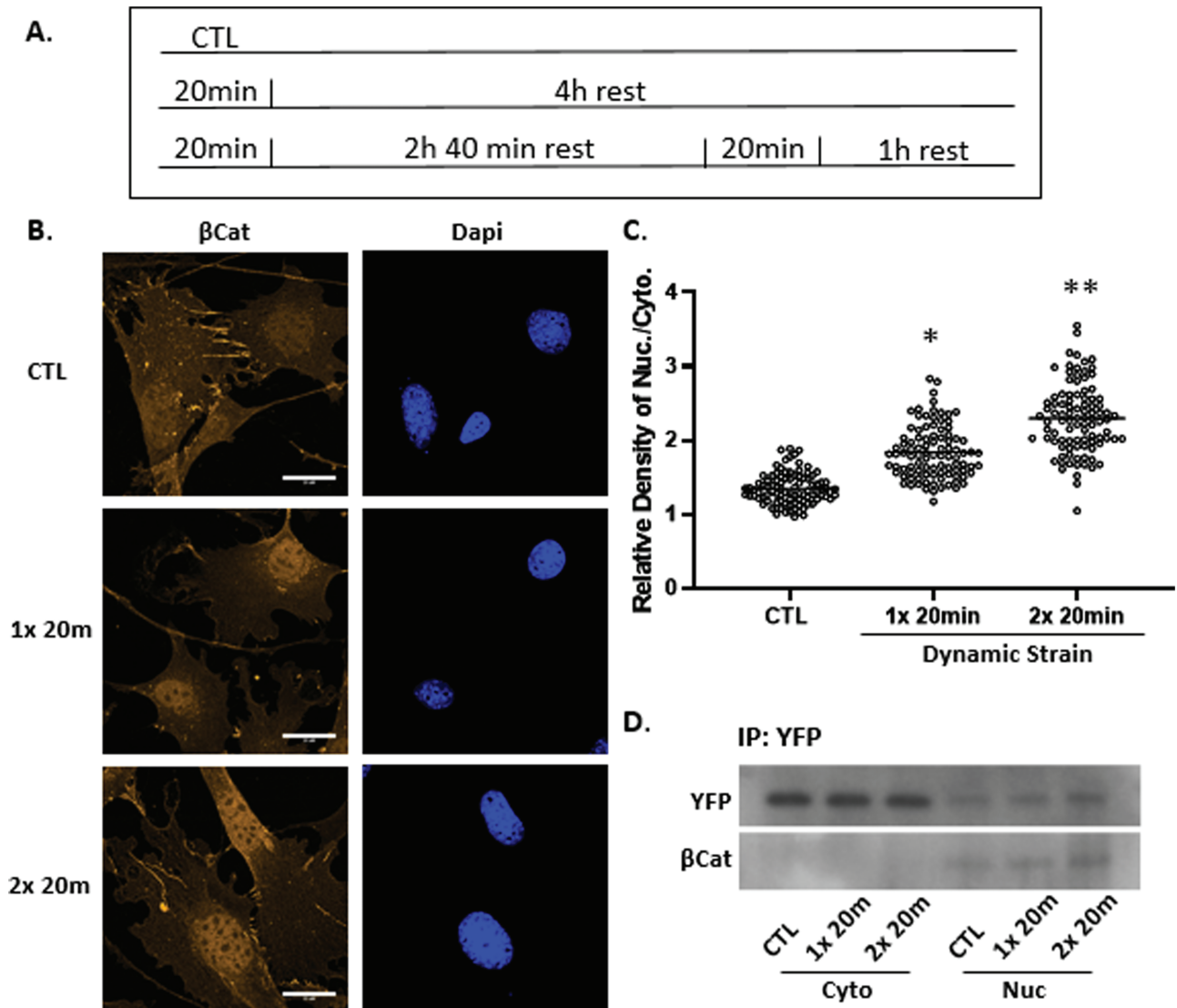
Figure 3. Nuclear β-catenin and actin rise further after a second dynamic strain bout. Timed application of strain for signal and double bouts (**A**). Mesenchymal stem cells were stained with anti-β-catenin (yellow) or DAPI (blue) showing increased β-catenin signal after the second strain bout, scale bar = 25 μm (**B**). β-catenin was quantified using ImageJ; statistical significance indicated by letter a and b, both = $P < .0001$ and $* \neq **$ (**C**). Nuclear and cytoplasmic fractions were pulled down with GFP Ab, and Western as shown for YFP and β-catenin, both of which increase after strain application (**D**).

β-catenin in the nucleus and the level of these complexes increased further after the second bout (Fig. 3D). In contrast, immunoprecipitation of cytoplasmic YFP-actin did not result in visible β-catenin, perhaps due to cytoplasmic sequestration of β-catenin. These data indicate that β-catenin entry into the nucleus is associated with force-induced actin translocation.

β-Catenin Nuclear Entry Is Dependent on Active Actin Transport into the Nucleus

Actin transport into the nucleus depends on the co-transport with cofilin-1 and importin-9.[18,44] When *Cfn1* was depleted by siRNA knock-down, nuclear transport of β-catenin transport after dynamic strain was abolished, while still increased by strain in MSCs treated with the scrambled RNA control (192 ± 6.5% of control; Fig. 4A-C). Static strain increased nuclear β-catenin to 138 ± 5.5% compared with the unstrained condition in MSCs treated with scrambled RNA. Again,

this smaller increase in nuclear β-catenin levels was not observed after *Cfn1* knockdown. There were no effects of *Cfn1* knockdown on static strain levels of nuclear β-catenin, which remained unchanged in both transfection conditions. We next knocked down *Ipo9*, which participates in the nuclear transport of many cargoes including histones[45,46] while also acting an obligate cofactor of cofilin-1 in actin transfer[47] (Fig. 4D-F). The accumulation of nuclear β-catenin due to dynamic strain evident in cells transfected with scrambled siRNA (158 ± 4% compared with control) was completely abolished after *Ipo9* knock down. There was no effect of *Ipo9* knock down on cytosolic β-catenin in the static condition. As anticipated, nuclear transport of YFP-actin-NLS which occurred after dynamic but not static strain, was abolished when *Cfn1* was knocked down (Supplementary Fig. S2). These results indicate that mechanically induced nuclear transport of β-catenin is mediated by molecular mechanisms that support nuclear entry of actin.
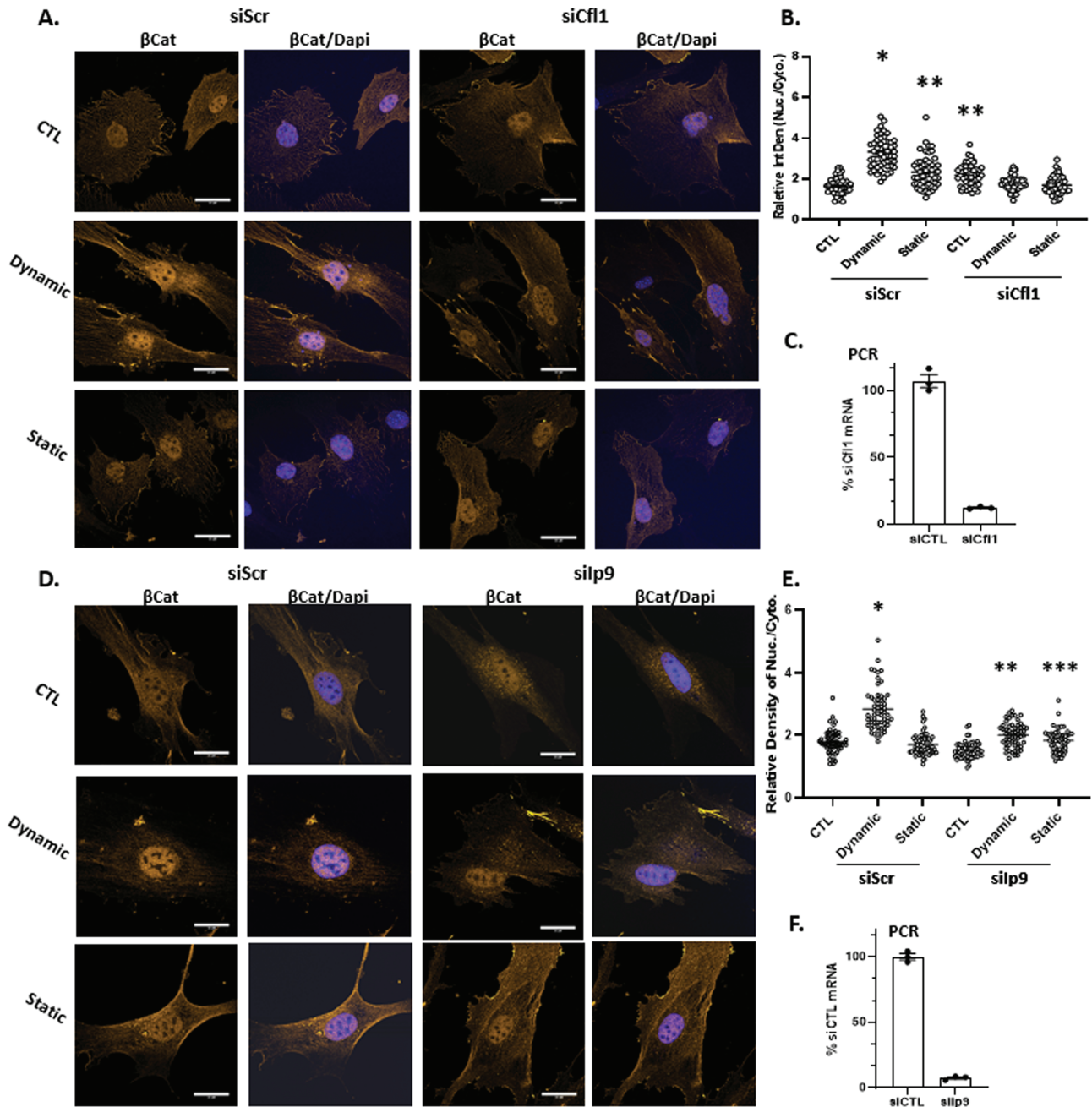
Figure 4. β-Catenin nuclear entry is dependent on active actin transport. Cofilin-1 or importin-9 were knocked down in MSC prior to treatment with dynamic or static strain. Three hours later, cells were stained with anti-β-catenin (yellow) and DAPI (blue) (**A** and **D**), scale bar = 25 μm. Nuclear intensity of β-catenin was analyzed by ImageJ program and statistical significance indicated by letter a, b, or c. (i). * ≠ **, $P < .0001$; (ii). ** ≠ ***; $P < .05$ (**B** and **E**). Real-time PCR indicated knock-down of *Cfl1* or *Ipo9* (**C** and **F**).

YAP1, But Not β-Catenin, Accumulates in the Nucleus After LPA-Induced Cytoplasmic Actin Polymerization

Development of F-actin polymers in the cytoplasm due to substrate stiffness or spreading is associated with nuclear transfer of YAP1.[2,38] Induction of F-actin fibers in the cytoskeleton by ligand-activation of the G-protein-coupled lysophosphatidic acid receptor (LPAR1) also induces YAP1 activation.[12,48] Such cellular redistribution is consistent with the model that YAP1 is sequestered by G-actin and released upon actin polymerization. Similar to previous observations with bone marrow derived MSCs,[16] establishment of an F-actin cytoskeleton by LPA induction was reflected by phalloidin staining and accompanied by YAP1 transfer to the nucleus (193 ± 3.4% compared to control, Fig. 5A, B). In contrast, LPA ligand activation of LPAR1 and F-actin formation failed to induce relocation of β-catenin from its cytoplasmic and membrane sites into the nucleus. These results indicate that generation of a cytoplasmic actin cytoskeleton was not sufficient to promote nuclear transfer of β-catenin. Rather β-catenin gains access to the nucleus in association with mono- and dimeric actin in response to dynamic mechanical forces.
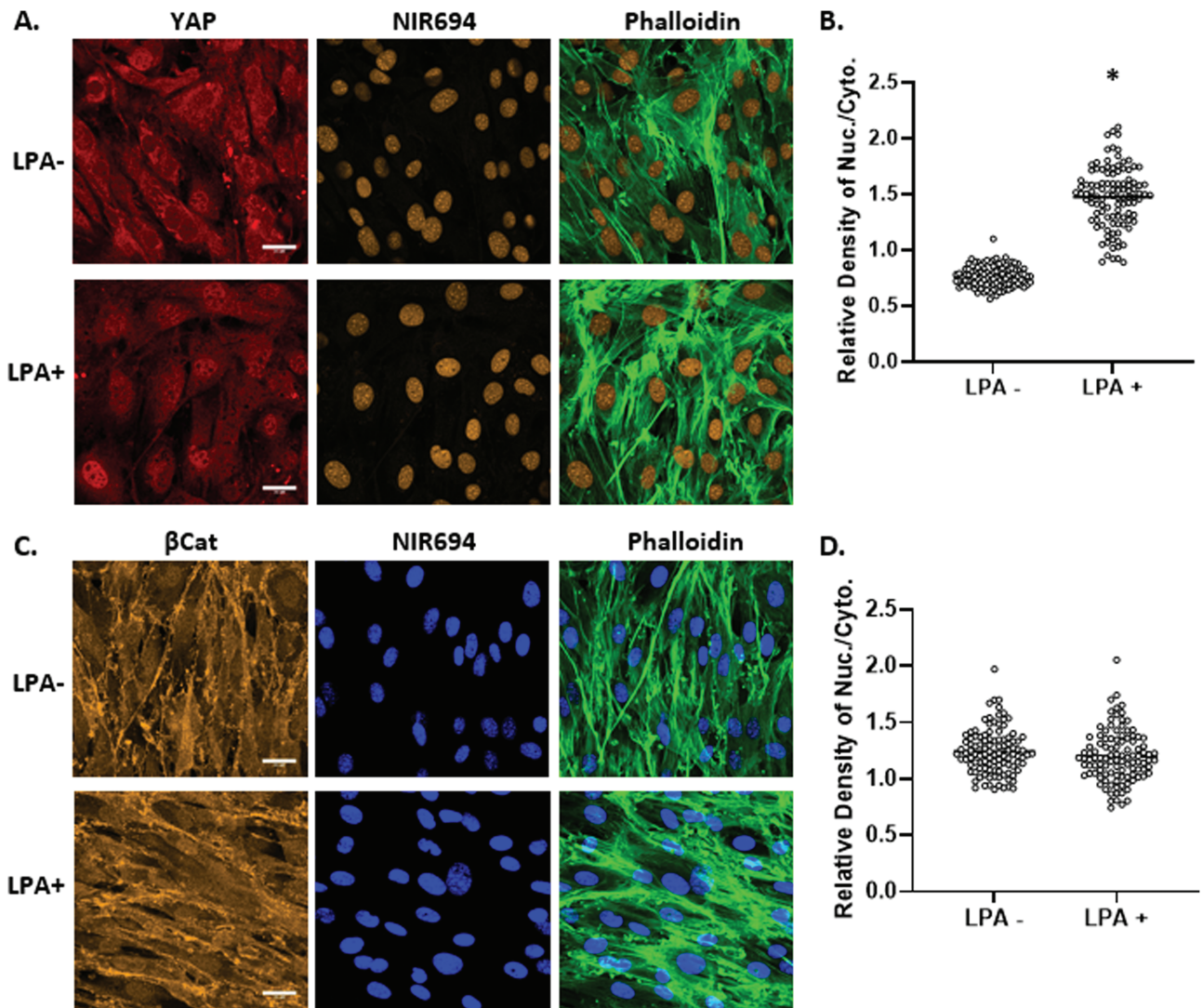
Figure 5. YAP1, but not β-catenin, responds to generation of cytoplasmic F-actin. Mesenchymal stem cells at 10 000 cells/cm² were treated with LPA (50 μM) for 24 hours and stained for YAP1 (red), nucleus (yellow), and F-actin (green) (**A**) or βCat (yellow), nucleus (blue), and F-actin (green), scale bar = 25 μm (**A, C**). Nuclear/cytoplasmic density of YAP1 or β-catenin IF was quantitated by ImageJ, * = $P < .0001$ (**B, D**).

Discussion

β-Catenin and YAP1 respond to alterations in the cellular mechanical environment with nuclear translocation and accumulation. The subcellular localization of both proteins is modulated by alterations in the cytoplasmic and nuclear actin state of the cell. Characteristics of the force applied affect these mechanoresponders differently, with dynamic substrate strains driving β-catenin into the nucleus, and static force promoting nuclear transfer of YAP1. Here we show in murine MSCs that nuclear transfer of β-catenin, but not YAP1, requires actin transfer into the nucleus generated by dynamic, but not static strain. Loss-of-function studies using siRNAs for *Cfn1* and *Ipo9* reveal that β-catenin transfer co-opts the mechanisms responsible for nuclear actin import.

Dynamic strain, through integrin attachments of the cell to substrate, leads to a signaling cascade in which focal adhesion kinase (FAK/PTK2) activates MTOR kinase (as part of the mTORC2 complex), which mediates AKT1 phosphorylation and the subsequent inactivation of GSK3β. The inhibition of GSK3β kinase activity not only protects β-catenin from proteasome destruction but also enhances

β-catenin appearance in the nucleus.[4,13] The mTORC2 complex and AKT1 also sequentially activate RhoGTPase[49] to reinforce the presence of signaling molecules at maturing focal adhesions.[7] Such recruitment of cellular proteins to sites of force amplifies actin remodeling[41] such that reapplication of strain, as shown here, further enhances β-catenin nuclear transfer. Importantly, we show here that dynamic strain generates actin flow into the nucleus. Availability of actin monomers for active transfer to the nucleus may influence the rate of actin remodeling.[50] Furthermore, dynamic strain may influence the iterative activation of RhoGTPase for actin monomer recycling.[36] This process differs from application of static stretch, where the generated cytoplasmic actin structure did not promote significant actin transfer into the nucleus. It is thus possible that nuclear import of actin was responsible for the greater nuclear modulus measured after dynamic, as compared to static, strain. Structural elements such as Lamin A/C[51] or LINC complex elements Sun 1 &2,[52] as well as chromatin compaction,[53] significantly contribute to nuclei stiffness. Low Intensity Vibration (LIV) which represents another

type of dynamic signal, increases isolated nuclear stiffness and leads to chromatin compaction without affecting LaminA/C and Sun proteins levels[37] suggesting that actin import may also contribute to chromatin organization.

Once inside the nucleus, actin and cofilin have been shown to together form rod structures, especially after mechanical stresses[54] such as dynamic strain. Formation of nuclear F-actin protects the nucleus from shape deformation, and promotes repair of incipient genetic damage.[55] Moreover, the tendency of actin to organize into secondary filaments can affect cell fate and lineage-progression of MSCs.[56] Thus it is likely that actin, along with β-catenin, might alter heterochromatin architecture and thus modulate transcription. Indeed, we have shown that mass actin transfer due to cytochalasin D treatment induces osteogenic differentiation of MSC,[18] perhaps in part through changes in the expression of Hippo pathway components (eg, VGLL4).[33] Furthermore, nuclear β-catenin is capable of preserving the self-renewing multipotent state of MSCs through activation of EZH2,[57,58] the enzymatic component of the polycomb repressive complex 2 (PRC2) that generates facultative heterochromatin through trimethylation of histone 3 lysine 25 (H3K27me3). In contrast YAP1, perhaps on a different temporal scale, sets a different regulatory potential for response to incoming signals, including availability of TEAD transcription factors[59] that can interact with the actin polymerization responsive protein VGGL4 which rises in response to cytochalasin D[33]. In addition, in MSCs, nuclear deformation itself can promote YAP1 nuclear localization, confirming that nuclear mechanics will affect cell function.[60] As such, the type of mechanical input—dynamic versus static—and the force induced effect on nuclear structure may pre-set either a β-catenin or YAP configuration to prime subsequent cellular responses to incoming signals.

In contrast to β-catenin, YAP1 exits the nucleus as actin flows inward due to cytochalasin D induced cytoplasmic F-actin depolymerization.[18] Stable cytoplasmic F-actin polymerization in response to a stiff substrate, on the other hand, leads to YAP1 nuclear translocation where F-actin forces on the nuclear surface cause flattening of the nucleus and opening of nuclear pores to support YAP1 transfer.[14] Here, LPA induction of cytoplasmic F-actin affected YAP1 but not β-catenin shuttling. Here our study showed that while dynamic strain increased both total cell and nuclear stiffness more than did static strain (~2-fold) it did not result in YAP1 nuclear entry. Dynamic low intensity vibration (LIV), in comparison, promoted YAP1 nuclear entry only when the cell stiffness increased by 4-fold.[16,61] These contrasting relationships to mechanical input highlight that β-catenin and YAP1 represent principal components of 2 functionally distinct and nonredundant pathways by which cytoskeletal mechanics modulate nuclear functions linked to proliferation and differentiation of stem cells.

It remains to be established how dynamic or static mechanical forces can influence MSC quality and potency via effects on nuclear entry of β-catenin or YAP. The effects of these 2 mechanoresponsive molecules (β-catenin and YAP) on MSC differentiation and function are contextual, and depend on multiple other contiguous and continuous variable in cells. Furthermore, another limitation of the *in vivo* work that we have presented here is that it is difficult to fully account for the complexity of the interactive elements that make up the skeleton, where force applied to one area can affect responses in distal bones, and the temporal aspects of bone remodeling by force responsive cells.

Nuclear import for β-catenin, YAP1, or β-actin occurs in the absence of classic NLS.[29,30] As such, all 3 proteins depend on other factors for targeted nuclear import, including association with structural elements and co-transporters. For example, disabling LINC complex function impedes mechanically-induced nuclear import of β-catenin under dynamic strain[17] and YAP1 under static strain.[62] Further, while YAP1 force-induced nuclear entry is independent of GTPase, inhibiting GTPases has been shown to decrease its nuclear accumulation.[14] TAZ which represents a YAP1 co-partner, does appear to have a non-canonical NLS which may affect YAP1 transfer.[30] Other studies have shown that YAP1 can be rapidly imported via interactions with transcription factors (eg, Runx2) that exhibit highly dynamic nuclear/cytoplasmic compartmentalization.[63,64] Nuclear import of actin requires cofilin/importin-9 interaction with monomeric and dimeric actin.[47] Because cofilin-1 does contain an NLS,[54] this protein enables actin nuclear transport in concert with importin-9; knockdown of either cofilin-1 or importin-9 blocks actin transport.[18] The latter finding was corroborated here by visualization of YFP-labeled actin. Here we present the novel finding that knockdown of either cofilin-1 or importin-9 also prevents nuclear transfer of β-catenin. This supports that nuclear import of β-catenin depends on strain-dependent interactions with mono- and dimeric actin shuttled into the nucleus through cofilin/importin-9 dependent mechanisms.

Conclusion

It is remarkable that 2 key molecules involved in controlling cell state decisions, β-catenin and YAP1, respond so specifically to different types of physical forces. A key question that emerges is how their presence in the nucleus controls cell function. In the case of MSCs, neither protein is linked to a clearly defined intracellular signaling pathway. We propose that β-catenin, through its association with actin dynamics, results in a structural orchestration of gene responses to the constant environmental barrage of incoming signals.

Funding

Conflict of Interest

The authors indicated no financial relationships.

Author Contributions

B.S., S.H.: conception and design, collection and assembly of data, data analysis, and interpretation, manuscript writing. Z.X.: collection and assembly of data, data analysis, and interpretation. M.S.: conception and design, financial support, manuscript writing. A.v.W., G.U., J.R.: conception and design, financial support, data analysis and interpretation, manuscript writing, final approval of manuscript.

Data Availability

The data underlying this article are available in the article and in its online supplementary material.

Supplementary Material

Supplementary material is available at *Stem Cells* online.

References

1. Sen B, Xie Z, Case N, et al. Mechanical strain inhibits adipogenesis in mesenchymal stem cells by stimulating a durable beta-catenin signal. *Endocrinology*. 2008;149:6065-6075. https://doi.org/10.1210/en.2008-0687.

2. Dupont S, Morsut L, Aragona M, et al. Role of YAP/TAZ in mechanotransduction. *Nature*. 2011;474:179-183. https://doi.org/10.1038/nature10137.

3. Wang S, Englund E, Kjellman P, et al. CCM3 is a gatekeeper in focal adhesions regulating mechanotransduction and YAP/TAZ signalling. *Nat Cell Biol*. 2021;23:758-770. https://doi.org/10.1038/s41556-021-00702-0.

4. Sen B, Styner M, Xie Z, et al. Mechanical loading regulates NFATc1 and beta-catenin signaling through a GSK3beta control node. *J Biol Chem*. 2009;284:34607-34617. https://doi.org/10.1074/jbc.M109.039453.

5. Lara-Castillo N, Kim-Weroha NA, Kamel MA, et al. In vivo mechanical loading rapidly activates beta-catenin signaling in osteocytes through a prostaglandin mediated mechanism. *Bone*. 2015;76:58-66. https://doi.org/10.1016/j.bone.2015.03.019.

6. Lewis KJ, Yi X, Wright CS, et al. The mTORC2 component rictor is required for load-induced bone formation in late-stage skeletal cells. *JBMR Plus*. 2020;4:e10366. https://doi.org/10.1002/jbm4.10366.

7. Sen B, Xie Z, Case N, et al. mTORC2 regulates mechanically induced cytoskeletal reorganization and lineage selection in marrow-derived mesenchymal stem cells. *J. Bone Mineral Res*. 2014;29:78-89.

8. Lombardi ML, Jaalouk DE, Shanahan CM, et al. The interaction between nesprins and sun proteins at the nuclear envelope is critical for force transmission between the nucleus and cytoskeleton. *J Biol Chem*. 2011;286:26743-26753. https://doi.org/10.1074/jbc.M111.233700.

9. Meng Z, Qiu Y, Lin KC, et al. RAP2 mediates mechanoresponses of the Hippo pathway. *Nature*. 2018;560:655-660. https://doi.org/10.1038/s41586-018-0444-0.

10. Koike M, Shimokawa H, Kanno Z, et al. Effects of mechanical strain on proliferation and differentiation of bone marrow stromal cell line ST2. *J Bone Miner Metab*. 2005;23:219-225. https://doi.org/10.1007/s00774-004-0587-y.

11. Shreberk-Shaked M, Oren M. New insights into YAP/TAZ nucleo-cytoplasmic shuttling: new cancer therapeutic opportunities?. *Mol Oncol*. 2019;13:1335-1341. https://doi.org/10.1002/1878-0261.12498.

12. Yu FX, Zhao B, Panupinthu N, et al. Regulation of the Hippo-YAP pathway by G-protein-coupled receptor signaling. *Cell*. 2012;150:780-791. https://doi.org/10.1016/j.cell.2012.06.037.

13. Case N, Thomas J, Sen B, et al. Mechanical regulation of glycogen synthase kinase 3beta (GSK3beta) in mesenchymal stem cells is dependent on Akt protein serine 473 phosphorylation via mTORC2 protein. *J Biol Chem*. 2011;286:39450-39456. https://doi.org/10.1074/jbc.M111.265330.

14. Elosegui-Artola A, Andreu I, Beedle AEM, et al. Force triggers YAP nuclear entry by regulating transport across nuclear pores. *Cell*. 2017;171:1397-1410.e14. https://doi.org/10.1016/j.cell.2017.10.008.

15. Touchstone H, Bryd R, Loisate S, et al. Recovery of stem cell proliferation by low intensity vibration under simulated microgravity requires intact LINC complex. *npj Microgravity*. 2019;5:11. https://doi.org/10.1038/s41526-019-0072-5.

16. Thompson M, Woods K, Newberg J, et al. Low-intensity vibration restores nuclear YAP levels and acute YAP nuclear shuttling in mesenchymal stem cells subjected to simulated microgravity. *npj Microgravity*. 2020;6:35. https://doi.org/10.1038/s41526-020-00125-5.

17. Uzer G, Bas G, Sen B, et al. Sun-mediated mechanical LINC between nucleus and cytoskeleton regulates betacatenin nuclear access. *J Biomech*. 2018;74:32-40. https://doi.org/10.1016/j.jbiomech.2018.04.013.

18. Sen B, Xie Z, Uzer G, et al. Intranuclear actin regulates osteogenesis. *Stem Cells*. 2015;33:3065-3076. https://doi.org/10.1002/stem.2090.

19. Greenbaum A, Chan KY, Dobreva T, et al. Bone CLARITY: clearing, imaging, and computational analysis of osteoprogenitors within intact bone marrow. *Sci Transl Med*. 2017;9:eaah6518. https://doi.org/10.1126/scitranslmed.aah6518

20. Tikhonova AN, Dolgalev I, Hu H, et al. The bone marrow microenvironment at single-cell resolution. *Nature*. 2019;569:222-228. https://doi.org/10.1038/s41586-019-1104-8.

21. Shen B, Tasdogan A, Ubellacker JM, et al. A mechanosensitive peri-arteriolar niche for osteogenesis and lymphopoiesis. *Nature* 2021;591:438-444. https://doi.org/10.1038/s41586-021-03298-5.

22. Rubin C, Lanyon L. Regulation of bone formation by applied dynamic loads. *J Bone Joint Surgery*. 1984;66A:397-402.

23. Ozcivici E, Luu YK, Adler B, et al. Mechanical signals as anabolic agents in bone. *Nat Rev Rheumatol*. 2010;6:50-59. https://doi.org/10.1038/nrrheum.2009.239.

24. Pagnotti GM, Styner M, Uzer G, et al. Combating osteoporosis and obesity with exercise: leveraging cell mechanosensitivity. *Nat Rev Endocrinol*. 2019;15(6):339-355.

25. Sankaran J, Uzer G, van Wijnen AJ, et al. Gene regulation through dynamic actin control of nuclear structure. *Exp Biol Med (Maywood)*. 2019;244:1345-1353. https://doi.org/10.1177/1535370219850079.

26. Benham-Pyle BW, Pruitt BL, Nelson WJ. Mechanical strain induces E-cadherin-dependent Yap1 and beta-catenin activation to drive cell cycle entry. *Science*. 2015;348:1024-1027. https://doi.org/10.1126/science.aaa4559.

27. Sen B, Paradise CR, Xie Z, et al. beta-Catenin preserves the stem state of murine bone marrow stromal cells through activation of EZH2. *J Bone Miner Res*. 2020;35:1149-1162.

28. Koike M, Kose S, Furuta M, et al. beta-Catenin shows an overlapping sequence requirement but distinct molecular interactions for its bidirectional passage through nuclear pores. *J Biol Chem*. 2004;279:34038-34047. https://doi.org/10.1074/jbc.M405821200.

29. Tolwinski NS, Wieschaus E. A nuclear function for armadillo/beta-catenin. *PLoS Biol*. 2004;2:E95.

30. Kofler M, Speight P, Little D, et al. Mediated nuclear import and export of TAZ and the underlying molecular requirements. *Nat Commun*. 2018;9:4966. https://doi.org/10.1038/s41467-018-07450-0.

31. Peister A, Mellad JA, Larson BL, et al. Adult stem cells from bone marrow (MSCs) isolated from different strains of inbred mice vary in surface epitopes, rates of proliferation, and differentiation potential. *Blood*. 2004;103:1662-1668. https://doi.org/10.1182/blood-2003-09-3070.

32. Case N, Xie Z, Sen B, et al. Mechanical activation of beta-catenin regulates phenotype in adult murine marrow-derived mesenchymal stem cells. *J Orthopaedic Res*. 2010;28:1531-1538.

33. Samsonraj RM, Paradise CR, Dudakovic A, et al. Validation of osteogenic properties of cytochalasin D by high-resolution RNA-sequencing in mesenchymal stem cells derived from bone marrow and adipose tissues. *Stem Cells Dev*. 2018;27:1136-1145. https://doi.org/10.1089/scd.2018.0037.

34. Guo Q, Xia Y, Sandig M, et al. Characterization of cell elasticity correlated with cell morphology by atomic force microscope. *J Biomech*. 2012;45:304-309. https://doi.org/10.1016/j.jbiomech.2011.10.031.

35. Hermanowicz P, Sarna M, Burda K, et al. AtomicJ: an open source software for analysis of force curves. *Rev Sci Instrum*. 2014;85:063703. https://doi.org/10.1063/1.4881683.

36. Sen B, Guilluy C, Xie Z, et al. Mechanically induced focal adhesion assembly amplifies anti-adipogenic pathways in mesenchymal stem cells. *Stem Cells*. 2011;29:1829-1836. https://doi.org/10.1002/stem.732.

37. Newberg J, Schimpf J, Woods K, et al. Isolated nuclei stiffen in response to low intensity vibration. *J Biomech*. 2020;110012. https://doi.org/10.1016/j.jbiomech.2020.110012.

38. Aragona M, Panciera T, Manfrin A, et al. A mechanical checkpoint controls multicellular growth through YAP/TAZ regulation by actin-processing factors. *Cell*. 2013;154:1047-1059. https://doi.org/10.1016/j.cell.2013.07.042.

39. Baarlink C, Grosse R. Formin' actin in the nucleus. *Nucleus*. 2014;5:15-20. https://doi.org/10.4161/nucl.28066.

40. Walker M, Rizzuto P, Godin M, et al. Structural and mechanical remodeling of the cytoskeleton maintains tensional homeostasis in 3D microtissues under acute dynamic stretch. *Sci Rep*. 2020;10:7696. https://doi.org/10.1038/s41598-020-64725-7.

41. Massou S, Nunes Vicente F, Wetzel F, et al. Cell stretching is amplified by active actin remodelling to deform and recruit proteins in mechanosensitive structures. *Nat Cell Biol*. 2020;22:1011-1023. https://doi.org/10.1038/s41556-020-0548-2.

42. Yamada S, Pokutta S, Drees F, et al. Deconstructing the cadherin-catenin-actin complex. *Cell*. 2005;123:889-901. https://doi.org/10.1016/j.cell.2005.09.020.

43. Yamazaki S, Yamamoto K, de Lanerolle P, et al. Nuclear F-actin enhances the transcriptional activity of beta-catenin by increasing its nuclear localization and binding to chromatin. *Histochem Cell Biol*. 2016;145:389-399. https://doi.org/10.1007/s00418-016-1416-9.

44. Huet G, Skarp KP, Vartiainen MK. Nuclear actin levels as an important transcriptional switch. *Transcription*. 2012;3:226-230. https://doi.org/10.4161/trns.21062.

45. Palacios V, Kimble GC, Tootle TL, et al. Importin-9 regulates chromosome segregation and packaging in Drosophila germ cells. *J Cell Sci*. 2021;134:jcs258391. https://doi.org/10.1242/jcs.258391.

46. Padavannil A, Sarkar P, Kim SJ, et al. Importin-9 wraps around the H2A-H2B core to act as nuclear importer and histone chaperone. *Elife*. 2019;8:e43630. https://doi.org/10.7554/eLife.43630

47. Dopie J, Skarp KP, Rajakyla EK, et al. Active maintenance of nuclear actin by importin 9 supports transcription. *Proc Natl Acad Sci USA*. 2012;109:E544-E552. https://doi.org/10.1073/pnas.1118880109.

48. Plessner M, Grosse R. Extracellular signaling cues for nuclear actin polymerization. *Eur J Cell Biol*. 2015;94:359-362.

49. Thompson WR, Guilluy C, Xie Z, et al. Mechanically activated Fyn utilizes mTORC2 to regulate RhoA and adipogenesis in mesenchymal stem cells. *Stem Cells*. 2013;31:2528-2537. https://doi.org/10.1002/stem.1476.

50. Carlier MF, Shekhar S. Global treadmilling coordinates actin turnover and controls the size of actin networks. *Nat Rev Mol Cell Biol*. 2017;18:389-401. https://doi.org/10.1038/nrm.2016.172.

51. Kennedy Z, Newberg J, Goelzer M, et al. Modeling stem cell nucleus mechanics using confocal microscopy. *Biomech Model Mechanobiol*. 2021;20:2361-2372.

52. Neelam S, Chancellor TJ, Li Y, et al. Direct force probe reveals the mechanics of nuclear homeostasis in the mammalian cell. *Proc Natl Acad Sci USA*. 2015;112:5720-5725. https://doi.org/10.1073/pnas.1502111112.

53. Stephens AD, Liu PZ, Banigan EJ, et al. Chromatin histone modifications and rigidity affect nuclear morphology independent of lamins. *Mol Biol Cell*. 2018;29:220-233. https://doi.org/10.1091/mbc.E17-06-0410.

54. Munsie LN, Desmond CR, Truant R. Cofilin nuclear-cytoplasmic shuttling affects cofilin-actin rod formation during stress. *J Cell Sci*. 2012;125:3977-3988. https://doi.org/10.1242/jcs.097667.

55. Lamm N, Read MN, Nobis M, et al. Nuclear F-actin counteracts nuclear deformation and promotes fork repair during replication stress. *Nat Cell Biol*. 2020;22:1460-1470. https://doi.org/10.1038/s41556-020-00605-6.

56. Sen B, Uzer G, Samsonraj RM, et al. Intranuclear actin structure modulates mesenchymal stem cell differentiation. *Stem Cells*. 2017;35:1624-1635. https://doi.org/10.1002/stem.2617.

57. Heo SJ, Thorpe SD, Driscoll TP, et al. Biophysical regulation of chromatin architecture instills a mechanical memory in mesenchymal stem cells. *Sci Rep*. 2015;5:16895. https://doi.org/10.1038/srep16895.

58. Sen B, Paradise CR, Xie Z, et al. beta-Catenin preserves the stem state of murine bone marrow stromal cells through activation of EZH2. *J Bone Mineral Res*. 2020;35:1149-1162.

59. Zhao B, Li L, Wang L, et al. Cell detachment activates the Hippo pathway via cytoskeleton reorganization to induce anoikis. *Genes Dev*. 2012;26:54-68. https://doi.org/10.1101/gad.173435.111.

60. Cosgrove BD, Loebel C, Driscoll TP, et al. Nuclear envelope wrinkling predicts mesenchymal progenitor cell mechano-response in 2D and 3D microenvironments. *Biomaterials*. 2021;270:120662. https://doi.org/10.1016/j.biomaterials.2021.120662.

61. Newberg J, Schimpf J, Woods K, et al. Isolated nuclei stiffen in response to low intensity vibration. *J Biomech*. 2020;111:110012. https://doi.org/10.1016/j.jbiomech.2020.110012.

62. Driscoll Tristan P, Cosgrove Brian D, Heo S-J, et al. Cytoskeletal to nuclear strain transfer regulates YAP signaling in mesenchymal stem cells. *Biophys J*. 2015;108:2783-2793.

63. Pockwinse SM, Rajgopal A, Young DW, et al. Microtubule-dependent nuclear-cytoplasmic shuttling of Runx2. *J Cell Physiol*. 2006;206:354-362. https://doi.org/10.1002/jcp.20469.

64. Zaidi SK, Sullivan AJ, Medina R, et al. Tyrosine phosphorylation controls Runx2-mediated subnuclear targeting of YAP to repress transcription. *EMBO J*. 2004;23:790-799. https://doi.org/10.1038/sj.emboj.7600073.